JOURNAL OF MATERIALS SCIENCE 29 (1994) 3023–3030

Percolation and damage behaviour in materials with liquid grain boundaries

F. BORDEAUX, M. C. DANG, B.BAUDELET
Génie Physique et Mécanique des Matériaux, Unité Associée au CNRS, Institut National Polytechnique de Grenoble, ENSPG, BP46, 38402 Saint Martin d'Hères, France

Percolation of the liquid phase and the damage behaviour in an aluminium alloy with liquid grain boundaries were characterized in experiments performed in tension and compression. The effects of the local stresses (due to grain-boundary sliding and macroscopic stresses) on the percolation of the liquid phase and on cavity development are discussed. It was found that cavities always appear and grow in the intergranular liquid films. It is shown that the presence of liquid films facilitates cavity formation and specimen rupture, for test conditions inducing local stresses higher than a critical stress. In contrast, for local stresses below the critical stress for hole formation, the liquid phase appeared to allow easy accommodation of the deformation without any damage.

1. Introduction

The mechanical behaviour of materials exhibiting viscous or liquid grain boundaries has received considerable attention in the literature for the last twenty years [1–38]. This interest, due largely to the importance of the high-temperature deformation of technologically important ceramics [1–14], is also noteworthy in other materials, i.e. metallic alloys [15–24], ice [25–28], metal-matrix ceramics [29–31], alkaline salts [14, 32–35] and frozen soils [14, 36–38]. Liquid or viscous grain boundaries (GBs) may be observed when the chemical or structural nature of the phases in the GB is different to that of the grains.

In these papers, the rheological behaviour of such materials has been partially studied and it seemed to be affected by the distribution and quantity of liquid or viscous GBs. Nevertheless, few investigations have been involved in mechanism determinations. Pharr *et al.* have provided the most complete work in this field [14–17]. They showed enhanced creep strain rates when liquid GBs were present and when the GBs were sufficiently surrounded by liquid [14]. They suggested the relative importance of mechanisms such as joint lubrication and diffusion, and cavitation or percolation in the liquid phase as a function of wetting and solubility of the liquid GBs in the solid grain [14, 16, 33]. The authors also showed the influence of liquid GBs on the mechanical behaviour of an Al-7000 alloy [24]. Superplastic-type behaviour was demonstrated for low strain rates in compression when GB phases were liquid. For higher strain rates, compressive tests led to a large amount of damage. In addition, this damage was shown to be greatly reduced by the application of compressive hydrostatic pressure of the same order as the applied stress. In this condition, a superplastic behaviour also appeared.

The mechanisms leading to the damage observed in material with liquid or viscous GBs have attracted very little attention. Most studies actually deal with cavity nucleation and growth in viscous (i.e. amorphous) GBs of some ceramics because of the importance of their premature failure at high temperatures [9–14]. In these cases, cavities are always observed to occur entirely within the viscous GBs. One may suppose that the viscous film at two GBs or the pockets at multiple junctions may become sufficiently stressed by hydrostatic tension during the mechanical tests (due to the applied stresses and to the GB sliding [13]) to give rise to easy cavitation. Thus, Marion *et al.* [10] studied the mechanisms of cavity nucleation and growth depending on the stress level in liquid-phase sintered ceramics. Growth and coalescence of oblate holes along two GBs were demonstrated to be responsible for interface failure at the highest local stresses. At lower stresses, above a critical value for cavity nucleation, failure was considered to initiate by the formation of spherical holes at triple junctions which are depleted by viscous flow of glass into a neighbouring two-grain interface. Finally, cavity evolution was predicted to depend on continuous viscous flow (at intermediate stresses) or on solution-reprecipitation processes at lower stresses (see also [8]). Page *et al.* [11] also suggested a similar dependence of cavity nucleation and growth on the stress level in hot-pressed SiC. Furthermore, they showed the very rapid cavity nucleation in limited nucleation sites so that the failure essentially involved cavity growth and coalescence [11].

As far as liquid GBs are concerned, the most interesting results on damage development and percolation were obtained by Pharr *et al.* on the metallic Cu–Bi system [14, 16] and on the alkaline-salt KCl [35]. The results obtained by these authors showed many similarities with the results given above on materials with viscous GBs in spite of some evident differences between the amorphous and liquid phases. Actually,

0022–2461

amorphous phases have a higher viscosity and a lower atomic diffusion than liquids. The easy percolation of the liquid phases observed by Pharr *et al.* on materials with liquid GBs is an illustration of such differences. In these cases, the liquid was observed to be rapidly expelled from the more compressed boundaries which are perpendicular to the applied compressive stress [16]. Following this rapid redistribution, the situation becomes rather similar to that described for amorphous GBs phases: the creep strain proceeded primarily by GB sliding accommodated by cavitation in the liquid at boundaries. Cavities were observed to nucleate in the liquid phases mainly at the triple junctions and to propagate across GB facets parallel to the applied stress under compression. It was also suggested that, once nucleated, cavities grow quite rapidly so that the cavity nucleation is rate limiting (note that the contrary was observed for amorphous GB phases [10]).

Consequently, because of the differences noted above, it appears that the results obtained on damage development in materials with amorphous GB phases cannot be directly extrapolated to materials with liquid interphases. In particular, the lack of relevant investigations of the influence of the local stresses on the damage development and percolation in materials with liquid GBs and the lack of information about the growing processes led us to study this behaviour under tension and compression for a model material. Finally, gaining an understanding of the rheological effects of liquid GBs phases is technologically important for sintering and forming with liquid phases.

2. Experimental procedure

The material studied was an aluminium alloy of the 7000 series prepared by OSPREY. The grains, whose size was about 30 μm, were approximately equiaxed and surrounded by a quaternary eutectic fusible at 477 °C [24]. This temperature is significantly lower than the melting temperature of the grains (around 630 °C) and, consequently, allows mechanical studies of the effects of the liquid GBs. Fig. 1 shows the initial microstructure of the alloy. Not all of the eutectic phases end up in the GBs. A significant fraction are actually trapped inside the grains during elaboration.

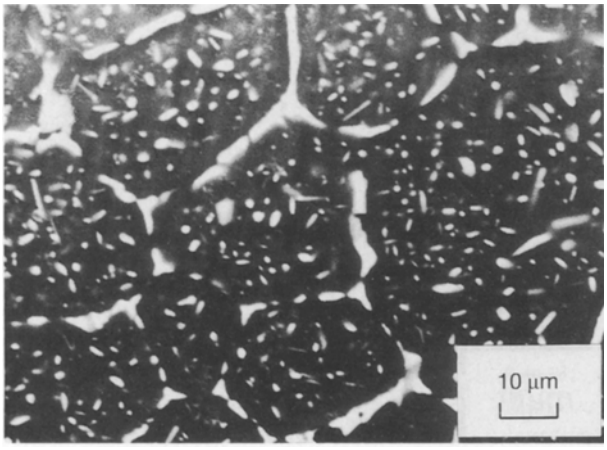

Figure 1 SEM micrograph of the microstructure of an as-prepared Al-7000 alloy. The eutectic phases can be seen at the grain boundary (white phase). A significant fraction is also trapped inside the grains.

Previous studies showed the progressive disappearance of the eutectic phases for long annealing periods at temperatures higher than the eutectic fusion temperature (T_{GB}) [24]. For example, only half of the initial eutectic phases remain after a 1 h anneal at 480 °C. Thus, the rheological test durations were limited to reducing such effects at these temperatures. On the other hand, only a slight evolution of the eutectic phases was observed at temperatures lower than T_{GB}, even for relatively long annealing periods. It is interesting to note that the thermal behaviour of this model material can be used to vary the thickness and distribution of the liquid GB by controlled annealings.

Compressive and tensile tests were conducted under an inert atmosphere with a mechanical testing machine equipped with a furnace with a quasi-constant temperature control in the material and during the tests with a maximum variation of $\pm 2°$.

3. Experimental results

3.1. Cavitation during compressive tests

Barrelling was always observed during the compressive tests in spite of the use of boron nitride sprayed on the contact surfaces to limit the friction. The stress states in the material are consequently rather complicated and include compressive, shear, radial and hoop stresses [39].

Cross-sections of Al-7000 alloys, quenched to ambient temperature after the compressive tests, were examined and compared to an undeformed reference specimen subjected to the same temperature conditions (Fig. 2). More liquid (white phase) is observed in the centre of the sample, where a combination of biaxial tension and uniaxial compression exists (Fig. 2c). Furthermore, the liquid quantity increases from the centre to the side of compressed specimens. In Fig. 2, the statistically higher proportion of liquid in GBs parallel to the axis of compression can be seen, these GBs being under perpendicular tensile stresses. On the contrary, a lower proportion of liquid is observed in GBs normal to the axis of compression. Furthermore, liquid phases are almost completely expelled from areas in triaxial compression (top and bottom of the sample, Fig. 2b). These results clearly indicate the existence of a network of channels between the pockets of liquid which allows the easy flow of the liquid phase (also called percolation). We have no experimental evidence about the flow rate of liquid eutectic phases, but can assume, following the results of Vaandrager and Pharr, that it is negligible compared to the duration of mechanical tests [16].

Fig. 3 shows the damage development under compression prior to the fracture observed in the central part of the sample. One can see that the liquid phase surrounds the grains incompletely and that some solid contacts exist between grains. The number of these contacts decreases from the centre to the side of the specimen where GBs are nearly totally wetted. The liquid GBs are also seen to smooth out the angles of the grains and consequently to change their shape

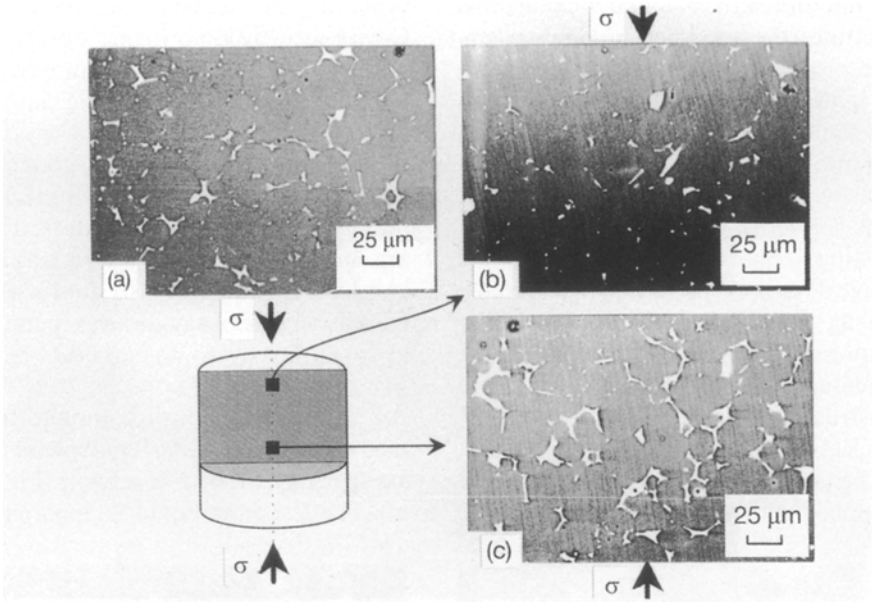

Figure 2 SEM micrographs illustrating the easy percolation of the liquid phase during compression at 480 °C, $\dot{\varepsilon} = 3 \times 10^{-4}\ s^{-1}$ for $\varepsilon = 0.05$: (a) the specimen without deformation under the same temperature conditions, (b) the zone near the specimen end (zone of triaxial compression), and (c) the central zone of the specimen (combination of compressive and tensile stresses).

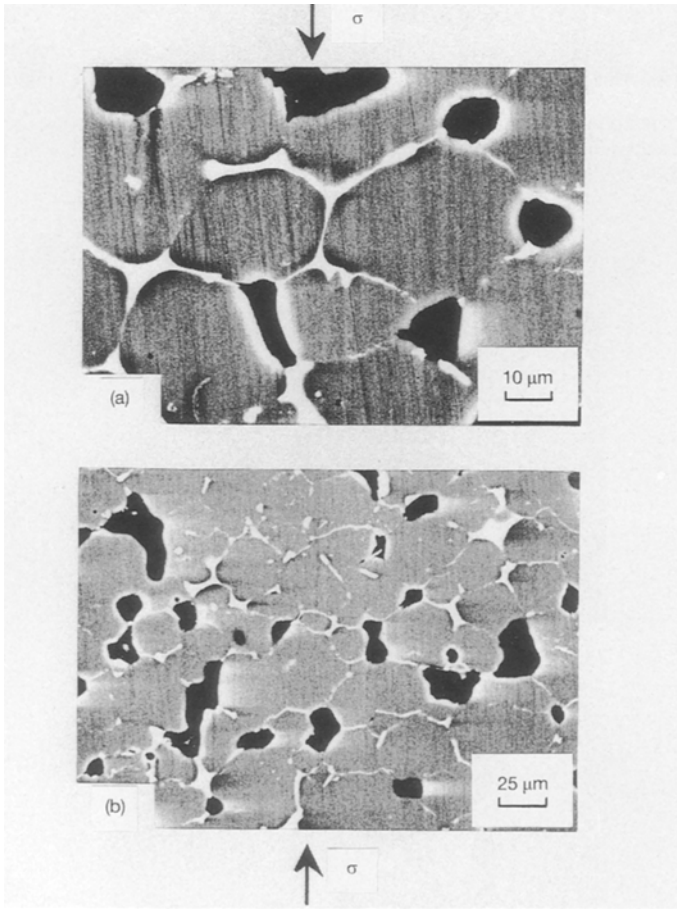

Figure 3 SEM micrographs showing cavities at multiple GBs (black areas) and coalescence along simple GBs after a compressive test at 480 °C, $\dot{\varepsilon} = 3 \times 10^{-4}\ s^{-1}$ and $\varepsilon = 0.3$.

significantly. Thus, the grain shape depends on the quantity of the surrounding liquid. All cavities apparently started at multiple junctions where liquid pockets existed. Some cavities have grown along grain facets which are roughly oriented parallel to the applied compressive stresses.

Fig. 4a illustrates the resulting failure after the complete coalescence of cavities that produces ball-like intergranular fracture surfaces in the side of the sample where there are higher proportions of liquid. The importance of the liquid quantity and distribution is illustrated by the observation of rupture surfaces in

other areas. The fracture surface actually changes as the fracture penetrates the specimen in zones where the grains are less surrounded by liquid and consequently where grains are more angular in shape (near the central zone). Fig. 4b shows such an area with some remaining facets, illustrating the solid contacts and the distribution of cavities concentrated at multiple junctions before rupture.

It is also interesting to note the effects of hydrostatic pressure on damage development. In a previous study, the authors actually showed that the application of hydrostatic compression considerably changed the mechanical behaviour of Al-7000 alloys with liquid GBs [24]. Microstructural study illustrates this effect on the cavity nucleation and growth and shows that the damage may be greatly reduced when hydrostatic compression is applied with a stress level of the same order as the applied compressive stresses (Fig. 5). Cavity growth is no longer observed when applying hydrostatic compression. However, some cavities do nucleate (see the arrows in Fig. 5a). Nevertheless, one cannot exclude any cavity nucleation associated with the shrinkage of liquid during cooling. Further statistical analysis will be necessary to eliminate all possible doubts. These results of hydrostatic-pressure effects are complementary to the calculation made for Cu–Bi systems with liquid Bi [16]. In this case, the calculated nucleation rate of cavities was found to increase when hydrostatic tension was applied.

3.2. Cavitation during tensile tests

Easy percolation of the liquid phase was also observed for specimens tested in tension (Fig. 6a). As for compressive tests, the liquid is apparently expelled from

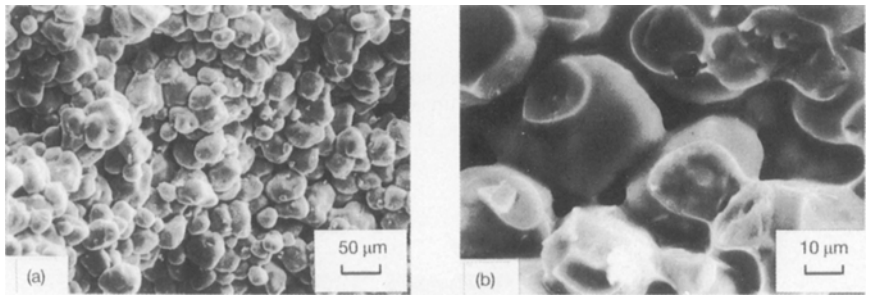

Figure 4 SEM micrographs of the intergranular fracture in: (a) the side of the specimen after compressive tests at 480 °C, $\dot{\varepsilon} = 3 \times 10^{-4}\ s^{-1}$ for $\varepsilon = 0.3$; (b) the bridges between cavities in areas where less liquid was present (near the central part of the sample) and consequently where GBs were not completely wetted by the liquid phases.

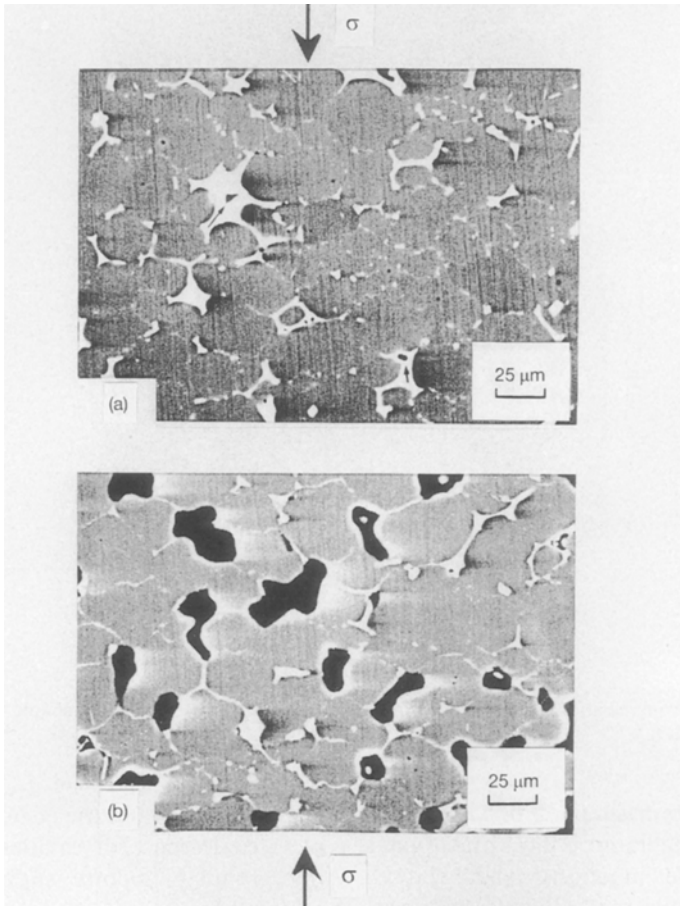

Figure 5 Comparison of damage produced under similar compressive test conditions (480 °C, $\dot{\varepsilon} = 3 \times 10^{-4}\ s^{-1}$, $\varepsilon = 0.3$) for different compressive hydrostatic pressures applied during the test: (a) 1 MPa, and (b) 0.1 MPa.

GBs under compression and attracted in GBs under tension (roughly perpendicular to the direction of the applied tension). No massive percolation at distances comparable to specimen dimensions was detected in tensile tests, compared to compressive tests. Nevertheless, a network of liquid-rich bands having a thickness of 2–3 grains is observed (see the broken lines in Fig. 6a). The bands cross each other perpendicularly and are roughly inclined at 45° with respect to the tensile axis. They are certainly zones of intensive shear. Furthermore, they seem to drain the liquid partially from volumes over a few to a few tens of grains. Cavities are seen to appear and develop in these bands inclined at 45° (see the arrow in Fig. 6a). Because of the apparently high cavity-growth rate (facets are entirely cavitated), it is impossible to determine whether they have nucleated at multiple-grain or at two-grain boundaries. Macroscopically, one may observe a saw-tooth fracture normal to the tension axis, that is, constituted of the many inclined coalesced cavities. SEM observations of the specimen surfaces (Fig. 6b) confirm the bulk behaviour with some additional features: the presence of a thin oxide layer at the sample surfaces actually acts as a tracer and outlines the surface deformations. They are parallel to the applied tension and mainly localized in the bands. Thus, the deformation may proceed initially from sliding in shear bands, followed by tensile deformation in the same bands before rupture. Examination of the fracture surface (Fig. 6c) shows the ball-shaped grains observed in compression. This grain shape is probably caused by the large quantity of liquid accumulated in the bands where failure occurs.

Mechanisms of cavity nucleation and growth consequently appear to be dependent on the quantity and distribution of the liquid phases. The most interesting results may be summarized as follows. (i) For tensile and compressive tests, cavities nucleate and grow in liquid GBs. (ii) Cavities grow at GBs roughly parallel to the applied stress in compression. The situation is rather different for tensile tests. Microscopically, the fracture actually follows the liquid-rich bands inclined at 45°. Macroscopically, the resulting failure is of a "saw-tooth" type and is perpendicular to the applied tension. (iii) Fractures are always intergranular, but grain shapes in the material and at the fracture surface appear to be strongly dependent on the quantity of liquid present at the GB before rupture (from ball-like grains in liquid-rich areas to more angular grain shapes in liquid-poor areas).

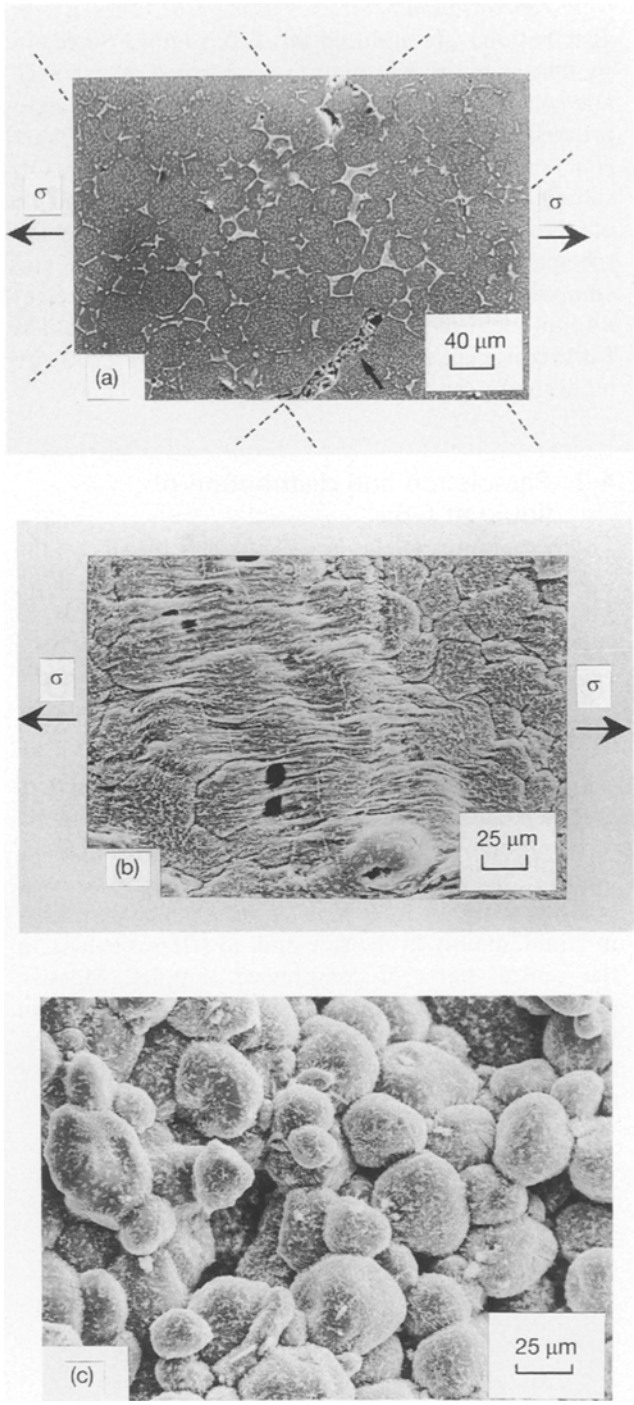

Figure 6 SEM micrographs of a specimen tested in tension at 480 °C, $\dot{\varepsilon} = 1.5 \times 10^{-5}\,s^{-1}$ for $\varepsilon = 0.2$ showing: (a) a section parallel to the sample surface, (b) the specimen surface, and (c) the intergranular fracture under the same test conditions.

4. Discussion

4.1. Stresses in the test specimens

Three different scales of stress variation influence the percolation in this material. They are as follows.

1. The macroscopic variation of stresses. This variation does not exist in tensile specimens, where the macroscopic tension is homogeneously distributed before the occurrence of instabilities. On the contrary, due to the specimen end constraints in compressed specimens which cause barrelling, the macroscopic stress pattern developed in a compression test piece is highly complex [39]. Essentially, while the stresses generated in the specimen end zones are nearly entirely compressive in nature, tensile hoop and radial stresses are produced in the body with the highest tensile stresses on the side of the sample.

2. The variation of stresses between adjacent GBs, due to GB orientations as compared to the applied stress. Maximum relative tensile stresses are actually expected in GBs perpendicular to the axis of tension or parallel to the applied compression. The maximum resulting stress gradients between adjacent GBs are consequently of the same order as the applied stress for both tensile and compressive tests.

3. The variation of stresses inside GBs. These stress distributions are induced by GB sliding. Since no significant grain deformation is observed after tensile and compressive tests, the deformation is concluded to proceed mainly by GB sliding. As proposed by Pharr *et al.*, the liquid at GBs may, furthermore, enhance GB sliding by lubrication [14, 16, 33]. The basic principle of GB sliding (GBS) and the resulting local stresses are schematically represented in Fig. 7 for tensile and compressive tests [10, 40, 41]. The grains themselves do not deform and slide rigidly over each other. Furthermore, the stress levels induced by GBS are higher than the applied stresses [39, 40].

4.2. Percolation and distribution of liquid at GBs

The percolation of the liquid phase is driven by the gradient of stresses in materials during deformation. The liquid actually tends to move from areas in compression to areas in tension. From the experimental results and stress studies (Section 4.1), the following three scales of liquid percolation may be deduced.

1. A massive percolation at distances comparable to specimen dimensions, due to the macroscopic stress distribution or deformation instabilities. This massive percolation is clearly observed in specimens tested in compression (Fig. 2). It induces areas which are richer in liquid, mainly in the side and, to a lesser extent, in the central parts of compressed samples. Massive percolation over smaller distances is also observed in tensile specimens when instabilities occur. Actually, the observed inclined bands indicate the tendency of the deformation to concentrate in shear zones. Such a phenomenon produces locally higher GBS and consequently higher associated tensile stresses (Fig. 7). As observed experimentally, the liquid content in these bands becomes consequently more important and the grains become completely surrounded by the liquid phase.

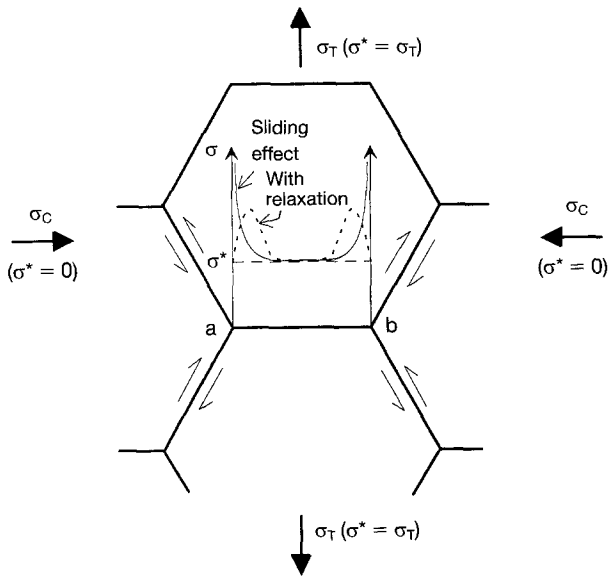

Figure 7 Schematic of the stress distribution along a two-grain junction (a–b), due to GBS, with and without relaxation at the multiple point. The maximum tensile stresses, schematically represented, are expected in GBs parallel to the axis of compression, σ_C or perpendicular to the axis of tension, σ_T. σ^*-values depend on the orientation of the GBs and on the test types. For the a–b GB, σ^* is equal to 0 and to σ_T, for compressive and tensile tests, respectively.

2. A local percolation at distances comparable to the grain size, due to the redistribution of the liquid phase from GB under compression to adjacent GB under tension or lower compression. This local percolation is expected to be similar for the specimens tested in tension and compression, due to similar stress gradients (see above).

3. A GB percolation due to the stress distribution along GBs (Fig. 7). As observed experimentally, it induces a larger quantity of liquid at multiple GBs where the tensile stresses are maximum. The incoming liquid releases the stresses in these areas. This GB percolation is observed for tensile and compressive specimens.

Finally, the resulting flow of liquid during tension and compression is a combination of the three modes of percolation described above.

Furthermore, the liquid percolation was demonstrated to be very rapid, for times which were negligible compared to the test duration [16]. Thus, it may easily be assumed that once the liquid has moved in large amounts from zones in compression to zones in tension (whenever possible), no liquid remains available for further macroscopic accommodation of the deformation by percolation. What happens locally is more complicated because one cannot exclude any percolation evolution due to geometrical changes (grain sliding and rotation) which may change the local stresses and open or close possible channels for the liquid flow.

When percolation occurs, it is also clear that the liquid disappears from some GBs and enters others where solid contacts apparently existed. The mechanism of penetration is not yet understood (it could be diffusion, dissolution–reprecipitation etc.). However, two driving forces may explain the opening of grain boundaries to allow the penetration of the liquid: (i) the local stress state acting on the GBs, as confirmed by the higher quantity of liquid in GBs perpendicular to local tensile stresses; and (ii) the good wetting of the liquid phase seen experimentally after annealings at temperatures higher than the fusion temperature of the eutectic phases (Figs 2–6).

The good wetting and chemical interactions of the liquid phases with the solid grains also lead to major modifications in grain shapes. This phenomenon, driven by the decrease of the liquid/solid surface energy, leads to ball-like grains in liquid-rich areas as observed in the sides of samples in compression (Fig. 4) and in the inclined bands in tensile specimens (Fig. 6). On the contrary, liquid-poor zones lead to more angular grain shapes.

4.3. Cavity evolution as a function of the stress state and liquid quantity

For materials with liquid GBs Marion *et al.* [10] also

observed the important role of GBS in materials with amorphous GBs. In addition, they stated that cavitation in liquid or viscous GB phases is induced by the depression (tensile stresses) at multiple GBs caused by the GBS. Consequently, they defined a critical tensile stress for hole formation, $\sigma^{C}_{CAV.}$ The same results were also obtained by Thouless and Evans [4] and confirmed by Pharr and Vaandrager on liquid GBs [14, 16]. In view of these results, it was interesting to obtain more qualitative information about the maximum local stress state at GB depending on the test conditions.

The following discussion considers qualitatively, the stress state in the liquid phase at GBS assuming that liquid percolation is no longer possible (that is, there is no more liquid available or the channels are closed). As schematically presented in Fig. 7, the sliding of planar boundaries induces a tensile-stress distribution near the grain edges. The combination of the local tensile stress due to GBS with the macroscopic compressive or tensile stress (σ_C and σ_T) leads, for the most stressed GBs in tension, to higher resulting local tensile stresses (σ_{GB}) during tensile tests (compared to compressive tests). Thus, as illustrated by the value of σ^* in Fig. 7:

$$\sigma_{GB} \text{ (tensile test)} > \sigma_{GB} \text{ (compressive test)}$$

When hydrostatic compression is additionally applied to the system during compressive tests, it decreases the maximum tensile stress on a GB by a value equal to the applied hydrostatic pressure. Finally, one can also write:

$$\sigma_{GB} \text{ (compressive test)} > \sigma_{GB} \text{ (compressive test + hydrostatic pressure)}$$

As seen before, the critical tensile stress ($\sigma^{C}_{CAV.}$) for hole formation within the liquid phase at multiple-grain or two-grain junctions may provide the basis for interpreting the cavity nucleation and growth. For local tensile stresses at GBs below the critical stress for cavity nucleation ($\sigma_{GB} < \sigma^{C}_{CAV.}$) the material should deform continuously without failure. Experimentally, this situation was observed during compressive tests at low strain rates (below or equal to $10^{-4}\ s^{-1}$). Under these conditions, the tensile stresses induced by GBS may be released by accommodation mechanisms (percolation of the liquid, diffusion in the liquid phase, etc.). At higher strain rates ($\geq 3 \times 10^{-4}\ s^{-1}$), failure always occurred [24]. This consequently places the level of the critical tensile stress for hole formation, $\sigma^{C}_{CAV.}$, in the range of the stresses induced by GBS alone (most of the tensile stresses in compression are due to GBS). Decreasing the maximum tension on GBs during compressive tests by applying hydrostatic compression may consequently avoid cavity nucleation and/or growth. This effect was actually observed experimentally for hydrostatic pressures higher than 0.5 MPa [24]. In contrast, as predicted above, cavitation was always observed during tensile tests, even for the lower strain rates used ($1.5 \times 10^{-5}\ s^{-1}$). The presence and the quantity of cavities consequently appear to be determined by the local tensile stresses in the liquid GB phase. In particular, the experimental results are consistent with the existence of a critical tensile stress for hole formation in the liquid, as defined by Marion *et al.* [10].

The role of the liquid quantity is evident when looking at the grain shape and fracture surfaces (Fig. 4). However, we have not, at the moment, any satisfactory explanation for its effects on cavity nucleation and growth. The damage under compression, for example, is more important in specimens with the lowest quantity of liquid GB phases [24]. That tends to prove that cavity formation is easier, due to the lower accommodation by percolation in the liquid-poor samples. More liquid actually implies a better accommodation of grain sliding and consequently lower tensile stresses in the liquid phase. At the same strain rates, increasing the liquid quantity leads to a superplastic-type behaviour without any damage [24]. On the other hand, when the quantities of liquid are too large all the solid bridges between the grains dissolve and the cohesion of the material is no longer maintained. Under such conditions, cavitation appears at low stresses, as observed on the sides of compressive specimens. The same results were also observed by the authors in aluminium alloys with 5 wt % Mg (grain size 30 μm) whose GBs were totally wetted by liquid gallium. This material was instantaneously broken, even under very low tensile stresses, without any plastic deformation. Thus, an optimum quantity of the liquid phase seems to be necessary to allow the easy deformation of the material without any damage formation.

5. Conclusion

We studied the damage behaviour of an Al-7000 alloy with liquid GBs. For this material, cavities were always seen to develop in the liquid films between grains. Since a GB facet was found to be either entirely cavitated or not cavitated at all, in the great majority of our observations, it has not been possible to conclude definitively on the cavity-nucleation site. Nevertheless, this phenomenon suggests that cavities grow quite rapidly once nucleated, and that cavity nucleation, rather than cavity growth, is rate limiting in our test conditions without hydrostatic compression.

Cavity development was observed to be strongly dependent on the local tensile stresses acting on GBs, due to GBS and macroscopic stresses. It was shown that the presence of liquid films facilitates cavity formation and specimen rupture for test conditions inducing local tensile stresses higher than a critical stress. In contrast, for local stresses below the critical stress for hole formation, the liquid phase appeared to allow easy accommodation of the deformation without any damage.

The stress distribution also induced very different percolations and consequently very different proportions of the liquid phase in the material, depending on the zones and the test conditions. The influence of the proportion of liquid on the damage development has not yet been clarified. However, the role of the liquid quantity was clearly seen when examining the grain shapes. The liquid actually changed their forms from

ball-like grains in liquid-rich areas, to more angular grains in areas with grains poorly surrounded by the liquid phase. As cavities and failures always develop in the liquid-richer areas, the fracture surface reproduces this ball-like geometry.

Acknowledgements

The authors would like to thank Pechiney-Voreppe for the supply of materials and D. Ferton for fruitful discussions. They also thank Dr T. G. Nguyen for technical support in the compressive tests under hydrostatic pressure.

References

1. K. H. CHAN, J. LANKFORD and R. A. PAGE, *Acta Metall.* **32** (1984) 1907.
2. R. L. TSAI and R. RAJ, *ibid.* **30** (1982) 1043.
3. A. G. EVANS and A. RANA, *ibid.* **28** (1980) 129.
4. M. D. THOULESS and A. G. EVANS, *ibid.* **34** (1986) 23.
5. F. F. LANGE, B. I. DAVIS and D. R. CLARKE, *J. Mater. Sci.* **15** (1980) 601.
6. D. R. CLARKE, *ibid.* **20** (1985) 1321.
7. R. M. ARONS and J. K. TIEN, *ibid.* **15** (1980) 2046.
8. R. RAJ and C. K. CHYUNG, *Acta Metall.* **29** (1981) 159.
9. R. MORRELL and K. H. G. ASHBEE, *J. Mater. Sci.* **8** (1973) 1253.
10. J. E. MARION, A. G. EVANS, M. D. DRORY and D. R. CLARKE, *Acta Metall.* **10** (1983) 1457.
11. R. A. PAGE, D. J. LANKFORD and S. SPOONER, *ibid.*, **32** (1984) 1275.
12. R. RAJ, *Colloque de Physique* **51** (1990) C1–393.
13. R. L. TSAI and R. RAJ, *Acta Metall.* **30** (1982) 1043.
14. G. M. PHARR, "Ashby symposium: the modelling of material behavior and its relation to design", edited by J. D. Embury and A. W. Thompson (TMS, London, 1990) p. 89.
15. B. L. VAANDRAGER and G. M. PHARR, *Scripta Metall.* **18** (1984) 1337.
16. *Idem., Acta Metall.* **37** (1989) 1057.
17. G. M. PHARR, P. S. GODAVARTI and B. L. VAANDRAGER, *J. Mater. Sci.* **24** (1989) 784.
18. M. C. ROTH, G. C. WEATHERLY and W. A. MILLER, *Acta Metall.* **28** (1980) 841.
19. D. D. PETROVIC, G. C. WEATHERLY and W. A. MILLER, *ibid.* **36** (1988) 2249.
20. A. WOLFENDEN and W. H. ROBINSON, *Acta Metall.* **25** (1977) 823.
21. D. WEBSTER, *Metall. Trans. A* **18** A (1987) 2181.
22. M. F. WEILL, PhD, Université Pierre et Marie Curie, Paris, (1979).
23. Y. S. NECHAEV, *Colloque de Physique C1, supplément au n° 1*, **51** (1990) 287.
24. B. BAUDELET, M. C. DANG and F. BORDEAUX, *Scripta Met. Mater.* **26** (1992) 573.
25. J. SCHWARZ and W. F. WEEKS, *J. Glaciology* **19** (1977) 499.
26. P. DUVAL, Proceedings of the Isotopes and Impurities in Snow and Ice, Grenoble, France, 1975. IAHS Publ. N° 118 (1977) p. 29.
27. P. S. GODAVARTI and G. M. PHARR, *J. Energy Res. Technol.* **107** (1985) 173.
28. L. LLIBOUTRY, *J. Glaciology* **10** (1971) 15.
29. T. G. NEIH and J. WADSWORTH, "*High strain rate superplasticity in metal matrix ceramics*", Lockheed internal report (Palo Alto, 1990).
30. O. D. SHERBY and J. WADSWORTH, *Prog. Mater. Sci.* **33** (1989) 169.
31. R. S. MISHRA and A. K. MUKHERJEE, *Scripta Metall.* **25** (1991) 271.
32. T. BAYKARA and G. M. PHARR, *Acta Metall.* **39** (1991) 1141.
33. G. M. PHARR and M. F. ASHBY, *ibid.* **31** (1983) 129.
34. R. SHEIKH and G. M. PHARR, *Scripta Metall.* **18** (1984) 837.
35. R. SHEIKH and G. M. PHARR, *Acta Metall.* **33** (1985) 231.
36. G. M. PHARR and J. E. MERWIN, *Cold Region Sci Technol.* **11** (1985) 205.
37. G. M. PHARR and P. S. GODAVARTI, *ibid.* **14** (1987) 273.
38. M. S. NIXON and G. M. PHARR, *J. Ener. Resour. Technol.* **106** (1984) 344.
39. R. W. EVANS and B. WILSHIRE, in "Creep of metals and alloys", edited by D. Mclean (Institute of Metals, London, 1985) p. 51.
40. J. CADEK, in "Creep in metallic materials" (Elsevier, New York, 1988) p. 279.
41. A. G. EVANS, J. R. RICE and J. P. HIRTH, *J. Amer. Ceram. Soc.* **63** (1980) 368.

Received 29 September 1992
and accepted 20 April 1993